Gastro Hep Advances 2023;2:221–231

ORIGINAL RESEARCH—BASIC

Regulation of Parietal Cell Homeostasis by Bone Morphogenetic Protein Signaling

Hidehiko Takabayashi,[1,*] Tuo Ji,[1,*] Lei Peng,[1,2] Xuan Li,[1,2] Masahiko Shinohara,[1] Maria Mao,[1] Kathryn A. Eaton,[3] Yatrik M. Shah,[4] and Andrea Todisco[1]

[1]Department of Internal Medicine, University of Michigan Medical Center, Ann Arbor, Michigan; [2]Department of Gastroenterology, First Affiliated Hospital of Nanjing Medical University, Nanjing, China; [3]Department of Microbiology and Immunology, University of Michigan Medical Center, Ann Arbor, Michigan; and [4]Department of Molecular and Integrative Physiology, University of Michigan Medical Center, Ann Arbor, Michigan

BACKGROUND AND AIMS: Loss of bone morphogenetic protein (BMP) signaling in the stomach, achieved by transgenic expression of the BMP inhibitor noggin (*H^+/K^+-Nog* mice), causes parietal cell (PC) loss, spasmolytic polypeptide-expressing metaplasia, a marker of preneoplasia, and activation of cell proliferation. We examined if specific inhibition of BMP signaling in PCs leads to aberrations in epithelial homeostasis. **METHODS:** Mice with floxed alleles of BMP receptor 1a (*$Bmpr1a^{flox/flox}$* mice) were crossed to *H^+/K^+-Cre* mice to generate *H^+/K^+-Cre;$Bmpr1a^{flox/flox}$* mice. Morphology of the mucosa was analyzed by hematoxylin and eosin staining. Distribution of H^+/K^+-ATPase-, IF-, and Ki-67-positive cells was analyzed by immunostaining. Expression of pit and neck cell mucins was determined by staining with the lectins Ulex Europaeus Agglutinin 1 and Griffonia (Bandeiraea) simplicifolia lectin II, respectively. Isolation of PCs from control and *Nog*-expressing mice was achieved by crossing *H^+/K^+-Nog* mice to *Rosa26-tdTomato* (Tom) mice to generate *H^+/K^+-Nog;Rosa26-tdTom* mice. *H^+/K^+-Cre* mice were then crossed to *H^+/K^+-Nog;Rosa26-tdTom* mice to generate *H^+/K^+-Cre;H^+/K^+-Nog;-Rosa26-tdTom* mice. Tom-labeled PCs were purified by flow cytometry. Changes in PC transcripts were measured by RNA-Seq. **RESULTS:** Six-month-old *H^+/K^+-Cre;$Bmpr1a^{flox/flox}$* mice exhibited increased epithelial cell proliferation, presence of transitional cells showing colocalization of IF with both Griffonia (Bandeiraea) simplicifolia lectin II-binding mucins and the H^+/K^+-ATPase, and expansion of Ulex Europaeus Agglutinin 1-positive cells. PC transcripts from Nog-expressing mice demonstrated induction of markers of Spasmolytic Polypeptide-Expressing Metaplasia. **CONCLUSION:** PC-specific loss of BMP signaling alters the homeostasis of the gastric epithelium leading to the development of metaplasia.

Keywords: Dysplasia; Differentiation; Metaplasia; RNA-Seq

Introduction

The gastric epithelium is a complex structure characterized by the presence of several types of highly specialized cells that belong to distinct differentiation pathways.[1] It has been suggested that perturbation of the homeostatic mechanisms that maintain the morphological and functional features of the gastric mucosa, as it occurs during chronic inflammation and injury, can induce aberrations in the normal programs of cell differentiation leading to metaplasia, dysplasia, and, ultimately, neoplastic transformation.[1,2] It appears that these events are initiated by the development of metaplastic changes of the gastric epithelium, such as those seen in intestinal metaplasia and spasmolytic polypeptide-expressing metaplasia (SPEM), a type of metaplasia characterized by the aberrant expression of spasmolytic polypeptide and of neck cell mucins at the base of the glands of the corpus.[1,2] According to some studies, SPEM might occur due to reprogramming of zymogenic cells in response to an epithelial injury and parietal cell loss. Indeed, several investigations have shown that loss of parietal cells is associated with profound abnormalities in the differentiation and development of multiple cell lineages.[3–11]

The bone morphogenetic proteins (BMPs) are regulatory peptides that exert important effects on the growth and differentiation of gastrointestinal tissues. The actions of the BMPs can be specifically blocked, in vivo, by inhibitory proteins, such as noggin that are expressed in tissues to modulate the level of activation of BMP signaling.[12]

The work from our laboratory has shown that in the stomach, BMP signaling exerts important regulatory effects on epithelial homeostasis. In particular, we demonstrated that transgenic expression of noggin in the mouse oxyntic mucosa leads to the development of SPEM, to parietal cell loss, and to increased epithelial cell proliferation. In addition, we noted that the gastric mucosa of the noggin-transgenic mice exhibits increased expression of growth factors and

*Hidehiko Takabayashi and Tuo Ji equally contributed to this work.

Abbreviations used in this paper: **BMP, bone morphogenetic protein; HBSS, Hank's Balanced Salt Solution; PC, parietal cell; QRT-PCR, quantitative real-time PCR; SPEM, spasmolytic polypeptide-expressing metaplasia.**

Most current article

2772-5723
https://doi.org/10.1016/j.gastha.2022.10.002

enhanced activation of mitogenic signaling mechanisms.[13] In support of a role of BMP signaling in the regulation of parietal cell homeostasis, we showed that incubation of cultured parietal cells with BMP-4 leads to stimulation of H^+/K^+-ATPase α-subunit gene expression and to enhancement of secretagogue-stimulated gastric acid production.[14]

The relevance of BMP signaling in gastric pathophysiology was further demonstrated by studies in which we reported that inhibition of BMP signaling in the stomach enhances *Helicobacter felis*- and *Helicobacter pylori*-induced inflammation, leading to the accelerated development of dysplasia, to increased expression and activation of oncogenic proteins such as AID and STAT3,[15] and to expansion of IF-expressing-Lgr5 progenitor cells.[16]

Because the role of the parietal cells in the development of metaplasia has been only partially elucidated, we undertook studies to test the hypothesis that inhibition of BMP signaling in the parietal cells leads to the development of metaplasia and to alterations in the normal programs of parietal cell differentiation. Toward this goal, we deleted BMP receptor 1a (*Bmpr1a*) in the parietal cells by crossing mice with floxed alleles of *Bmpr1a* ($Bmpr1a^{flox/flox}$ mice) to animals that express *Cre recombinase* under the control of the H/K-ATPase β-subunit gene promoter (H^+/K^+-*Cre* mice). Our studies demonstrate that parietal cell-specific loss of BMP signaling alters the homeostasis of the gastric epithelium, leading to the development of metaplasia and to alteration in the normal programs of parietal cell differentiation.

Material and Methods

Mice

The H^+/K^+-*noggin* (H^+/K^+-*nog*) transgenic mice were bred in our laboratory, and they were previously described.[13] Pathogen-free C57BL/6 mice and *Rosa26-tdTom* (*Rosa26-Tom*) mice aged 4–10 weeks were purchased from Jackson Laboratory (Bar Harbor, ME). The $Bmpr1a^{flox/flox}$ [17] mice were provided by the laboratory of Dr Yuji Mishina (University of Michigan). The H^+/K^+-*cre* mice in which the expression of *Cre* is driven by endogenous H^+/K^+-*ATP-ase* β *subunit* regulatory sequences were obtained from the laboratory of Dr Jeff Gordon.[18] Mouse genotyping was described elsewhere.[13] Specific inhibition of BMP signaling in parietal cells was achieved by crossing H^+/K^+-*cre* mice to $Bmpr1a^{flox-flox}$ mice to generate H^+/K^+-*cre;*$Bmpr1a^{flox-flox}$ mice. In order to perform an RNA-Seq analysis in parietal cells isolated from mice that express the BMP inhibitor noggin in the gastric mucosa, we crossed H^+/K^+-*Nog* mice to *Rosa26-tdTomato* reporter mice to generate H^+/K^+-*Nog;Rosa26-tdTom* mice. H^+/K^+-*Cre* mice were then crossed to both H^+/K^+-*Nog;Rosa26-tdTom* and *Rosa26-tdTom* mice to generate H^+/K^+-*Cre;*H^+/K^+-*Nog;Rosa26-tdTom* (HKNT) and H^+/K^+-*Cre;Rosa26-tdTom* (HKT) mice, which were used as controls. The mice were maintained on a C57BL/6 background. In all experiments, the animals were fasted overnight with free access to water before tissue collection. The mice were housed under specific pathogen-free conditions in automated watered and ventilated cages on a 12-hour light/dark cycle, in the animal maintenance facility at the University of Michigan. All animal experiments were approved by the University of Michigan Animal Care and Use Committee. Three- and six-month-old mice were used for analysis.

RNA Isolation and Quantitative Real-Time PCR Analysis

RNA was isolated from full-thickness samples of the corpus of mice using TRIzol reagent (Invitrogen), followed by DNase treatment and purification with the RNeasy Mini kit (Qiagen).[13] Quantitative real-time PCR (QRT-PCR) was performed according to previously published methods [13] using primer sequences and protocols that were obtained from commercially available sources. *Gapdh* and *Bmpr1a* primers were obtained from Integrated DNA Technologies (Coralville, IA). *Bmpr1a* QRT-PCR primers span exons 2–3 of the gene. The sequences include primer 5′-CTTGGCAATGACTTTCACCTG-3′ that binds in exon 3 (284–304 in Genebank NM-009758.4) and primer 5′-TCGCTTTGATACTGTCTTGGAA-3′ that binds in exon 2 (170–191 in Genebank NM-009758.4). The deletion in the *Bmpr1a* floxed mice obtained from the laboratory of Dr Yuji Mishina removes a portion of exon 2. Accordingly, these primers will not amplify a product in the recombined mice. The *Id2* primers were obtained from Qiagen (Valencia, CA). A QRT-PCR analysis of *Gif* and *Tff2* mRNA abundance was performed using previously described primers and methods.[19]

Gastric Epithelial Cell Isolation and Flow Cytometry

Fluorescence-activated cell sorting isolation of tomato-labeled parietal cells from HKNT mice and HKT mice was performed as previously described.[20] Samples of gastric mucosa were placed in Mg^{2+}- and Ca^{2+}-free Hank's Balanced Salt Solution (HBSS), 5% fetal bovine serum, and 2-mM ethylenediaminetetraacetic acid; shaken for 20 minutes at 37 °C; and filtered through a 100-μm cell strainer. After filtration, the samples were pelleted and resuspended in HBSS containing 0.1-U/ml Liberase (Roche, Basel, Switzerland) and 40-μg/ml DNase I (Sigma, St. Louis, MO). The solutions were shaken for 10 minutes at 37 °C, filtered through a 100-μm cell strainer, and spun at 1500 rpm for 5 minutes. After one wash with HBSS, the pellets were resuspended in HBSS, containing an aqua viability dye (LIVE/DEAD Fixable Aqua dead cell stain kit; Invitrogen, Carlsbad, CA) according to the manufacturer's instructions. After 1 wash, the cells were resuspended in HBSS containing 1% fetal bovine serum, filtered through a 50-μm filter (Partec/Sysmex, Lincolnshire, IL), and used for analysis. $Tomato^{+ve}$ cells were isolated using fluorescence-activated cell sorting. Analyses were performed using an iCyte Synergy (Sony Biotechnology, San Jose, CA) with WINLIST V.8 (Verity Software House, http://www.vsh.com) software. The laser emission wavelengths and filter used were 561-nm laser with a 577/25-nm filter. The aqua viability dye was excited with a 405-nm laser and detected with a 525/50-nm filter. The sorted cells were collected into sterile 1.5-ml tubes containing 300 μl of RNA lysis buffer and used for RNA extraction (Zymo Research, Irvine, CA).

Histochemical Analysis and Image Acquisition

Tissue fixation, generation of paraffin sections, hematoxylin and eosin staining, and immunostaining were performed

according to previously published methods.[13,15,19] Sections were stained with the following primary antibodies: anti-H^+/K^+-ATP-ase α-subunit (1:500) (Medical and Biological Laboratories, Nagoya, Japan, catalog number: DO31-3), anti-Ki-67 (1:500) (Thermo Fisher Scientific, Waltham, MA, catalog number: MA5-14520), and anti-intrinsic factor (1:1000) (gift from Dr Jason Mills, Washington University, St. Louis, MO). In some experiments, the slides were stained for 1.5 hours at 37 °C with Alexa 488-conjugated Griffonia (Bandeiraea) simplicifolia lectin II (GSII) (1:1000) (Vector Laboratories, Burlingame, CA, catalog number: FL-1211) and Alexa 555-conjugated Ulex Europaeus Agglutinin 1 (UEA1) lectin (1:200) (Vector Laboratories, Burlingame, CA, catalog number: FL-1061). For immunofluorescence analysis, Alexa 555-donkey antirabbit (1:500) and Alexa 488-donkey antirat and antimouse (1:500) secondary antibodies were used (Molecular Probes, Eugene, OR). ProLong Gold Antifade reagent with 4',6-Diamidino-2-phenylindole (Invitrogen, Carlsbad, CA) was used for nuclear counterstain and mounting medium. Control experiments were performed by incubating the slides in the presence of the secondary antibodies without the primary antibodies (data not shown). Visualization of the slides was performed with a Nikon Eclipse E 800 fluorescence microscope for all other studies.

For histologic analysis, sections from the stomachs of 3 to 4 separate animals from each of the 4 treatment groups were examined as previously described.[15,21] Slides containing sections of well-oriented gastric glandular mucosa were examined in a blinded fashion. Only fields that contained full-thickness gastric mucosa that was oriented perpendicularly were analyzed. All well-oriented fields were analyzed. Each field was examined separately for the presence or absence and severity of neutrophilic cell infiltration, gastritis, and epithelial metaplasia/dysplasia.[21] Glandular dysplasia was defined as an abnormal gland morphology including splitting, focally severe epithelial hyperplasia ("piling up"), and metaplasia. Cellular dysplasia was defined as the presence of cytoplasmic and/or of nuclear anomalies (size variation, binuclear cells), loss of polarity, and/or loss of basement membrane contact.[15,21]

The number of H^+K^+-ATP-ase α-subunit- and Ki-67-positive cells was determined by counting the number of stained cells in at least 8 to 10 fields in slides derived from 3 to 4 animals from each treatment group, using the Fiji imaging program (ImageJ).[22]

Data Analysis

Data are expressed as means ± standard error. Statistical analysis was performed using Student's t test. P values $< .05$ were considered to be significant.

RNA-Seq Analysis

Library preparation and sequencing was performed by the UM Advanced Genomics Core. The total RNA quality was assessed using the TapeStation 2200 (Agilent). At least 1 ng of DNase-treated total RNA was used to generate indexed mRNA libraries using SMART-Seq Ultra Low Input RNA-seq V3 kits (Takara). Library quality was assessed using the TapeStation 2200 (Agilent), and libraries were quantitated using KAPA Library Quantification Kits (Roche). Pooled libraries were subjected to 50-bp single-end sequencing according to the manufacturer's protocol (Illumina HiSeq 2500). bcl2fastq2 Conversion Software (Illumina) was used to generate demultiplexed Fastq files. The read files were downloaded from the Sequencing Core's storage at the University of Michigan Bioinformatics Core and concatenated into a single fastq file for each sample. The quality of the raw reads data for each sample was checked using FastQC (http://www.bioinformatics.bbsrc.ac.uk/projects/fastqc/) (version 0.10.0) to identify features of the data that may indicate quality problems (eg, low-quality scores, overrepresented sequences, inappropriate guanine/cytosine content). Three bases at the 5′ ends were trimmed to remove Clonetech adapter sequences and also for low-quality sequences. The Tuxedo Suite software package was used for alignment, differential expression analysis, and postanalysis diagnostics.[23–25] Briefly, reads were aligned to the reference genome including mRNAs (UCSC mm10) (http://genome.ucsc.edu/) using TopHat (version 2.0.9) and Bowtie (version 2.1.0.). The default parameter settings were used for alignment, with the exception of "–b2-very-sensitive" telling the software to spend extra time searching for valid alignments. FastQC was employed for a second round of quality control (postalignment) to ensure that only high-quality data would be input to expression quantitation and differential expression analysis. Cufflinks/CuffDiff (version 2.1.1) was utilized for expression quantitation, normalization, and differential expression analysis, using UCSC mm10.fa as the reference genome sequence. For this analysis, parameter settings "–multi-read-correct" were used to adjust expression calculations for reads that map in more than 1 locus, as well as "–compatible-hits-norm" and "–upper-quartile–norm" for normalization of expression values. Diagnostic plots were generated by using the CummeRbund R package.

Locally developed scripts were used to format and annotate the differential expression data output from CuffDiff. Briefly, genes and transcripts were identified as being differentially expressed based on 3 criteria: test status = "OK", FDR 0.05, and fold change $\geq \pm 1.5$. Genes and isoforms were annotated with NCBI Entrez GeneIDs and text descriptions.

The Molecular Signatures Database,[26] version 6, was used for enrichment analysis of sets of differentially expressed genes to identify significantly enriched functional categories.

The R Software (version 3.5.1; https://www.r-project.org) and the "pheatmap" R package (https://cran.r-project.org/web/packages/pheatmap/index.html) were used to cluster the expression of differentially expressed genes between parietal cells obtained from control mice (HKT mice) and those isolated from mice that expressed the BMP inhibitor Noggin in the gastric mucosa (HKNT mice).

Venn diagram analysis (http://bioinformatics.psb.ugent.be/webtools/Venn/) was used to determine the overlap between the transcripts expressed in our database and those listed in a published report of intestinal metaplasia- and SPEM-specific transcripts.[27] The RNA-seq data were deposited in the GEO repository, accession number GSE202355/https://www.ncbi.nlm.nih.gov/geo/query/acc.cgi?acc=GSE202355.

Results

In this manuscript, we tested the hypothesis that specific inhibition of BMP signaling in parietal cells alters parietal cell differentiation leading to aberrations in the normal homeostatic mechanisms of the gastric epithelium. Toward

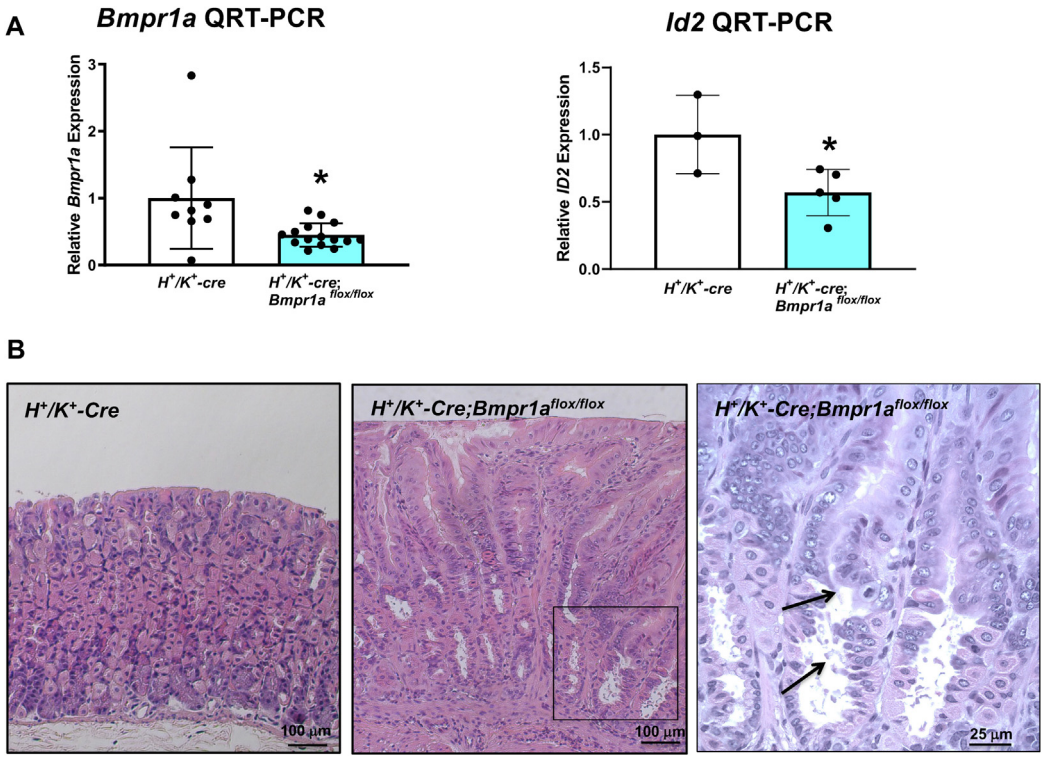

Figure 1. Generation and characterization of H^+/K^+-*Cre;Bmpr1a*$^{flox\text{-}flox}$ mice. (A) *Bmpr1a* and *Id2* mRNA signals in 3- to 5-month-old H^+/K^+-*Cre* mice were compared to those detected in H^+/K^+-*Cre;Bmpr1a*$^{flox\text{-}flox}$ mice of similar age using QRT-PCR. Values are shown as means ± standard error. *$P < .05$. (B) Representative H&E-stained paraffin sections of the mucosa of the corpus of six-month-old H^+/K^+-*Cre* and of H^+/K^+-*Cre;Bmpr1a*$^{flox\text{-}flox}$ mice. The magnified window depicts areas of dysplastic changes in H^+/K^+-*Cre;Bmpr1a*$^{flox\text{-}flox}$ mice. Size bars 100 μm and 25 μm in the window. Arrows point to areas of dysplastic epithelium. Similar abnormalities were identified in sections obtained from 4 other six-month-old H^+/K^+-*Cre;Bmpr1a*$^{flox\text{-}flox}$ mice.

this goal, we deleted BMP receptor 1A (*Bmpr1a*) in the parietal cells, by crossing mice expressing floxed alleles of *Bmpr1a* to H^+/K^+-*Cre* mice in which the expression of *Cre* is driven by the H^+/K^+-*ATP-ase β subunit* gene promoter, to generate H^+/K^+-*Cre;Bmpr1a*$^{flox\text{-}flox}$ mice. To confirm decreased expression of *Bmpr1a* and inhibition of BMP-dependent gene expression in the transgenic mice, we measured using QRT-PCR the expression of *Bmpr1a* and *Id2*, a well-characterized BMP-responsive gene,[28] in homogenates of full-thickness samples of fundic mucosa. As shown in Figure 1A, H^+/K^+-*Cre;Bmpr1a*$^{flox\text{-}flox}$ mice exhibited a significant decrease in the expression of both *Bmpr1a* and *Id2*, supporting the inhibition of BMP signaling.

We examined morphological changes induced by the diminished expression of *Bmpr1a* in the parietal cells. As shown in the representative H&E-stained sections obtained from six-month-old mice depicted in Figure 1B, the mucosa of the corpus of H^+/K^+-*Cre;Bmpr1A*$^{flox\text{-}flox}$ mice demonstrated prominent foci of epithelial hyperplasia, metaplasia, and focal glandular dysplasia, resulting in downward expansion of the apical compartment and of compression of the adjacent mucosa. No significant inflammation was seen. The changes involved the entire length of the glands, and they were present in all examined sections from six-month-old H^+/K^+-*cre;Bmpr1a*$^{flox/flox}$ mice. No difference in the extent or severity of the abnormalities between individual mice was seen. One to 2 foci of dysplasia were detected in each section.

In order to assess if inhibition of BMP signaling in the parietal cells causes alterations in parietal cell number and in the normal proliferative activity of the epithelium of the corpus, we analyzed the number of parietal and proliferating cells by immunostaining for the H^+,K^+-ATPase α-subunit and Ki-67. As shown in the histological sections of the corpus of six-month-old mice and in the bar graphs depicted in Figure 2, representing the number of positively stained cells, H^+K^+-*Cre;Bmpr1a*$^{flox\text{-}flox}$ mice demonstrated a marked decrease in the number of parietal cells (Figure 2A and B) and a robust increase in the number of proliferating cells with Ki-67-positive nuclei (Figure 2C and D), which could be seen both in the isthmus and at the base of the glands, when compared to control H^+/K^+-*cre* mice. Staining of sections of the corpus of six-month-old H^+K^+-*Cre;Bmpr1a*$^{flox\text{-}flox}$ mice with both anti-H^+,K^+-ATPase α-subunit and anti-Ki67 antibodies did not identify any Ki-67-positive nuclei in the parietal cells, suggesting that, in this system, H^+,K^+-ATPase α-subunit-expressing cells do not proliferate (Figure 2E).

In contrast to these observations, no abnormalities in mucosal morphology, cell proliferation, and the distribution

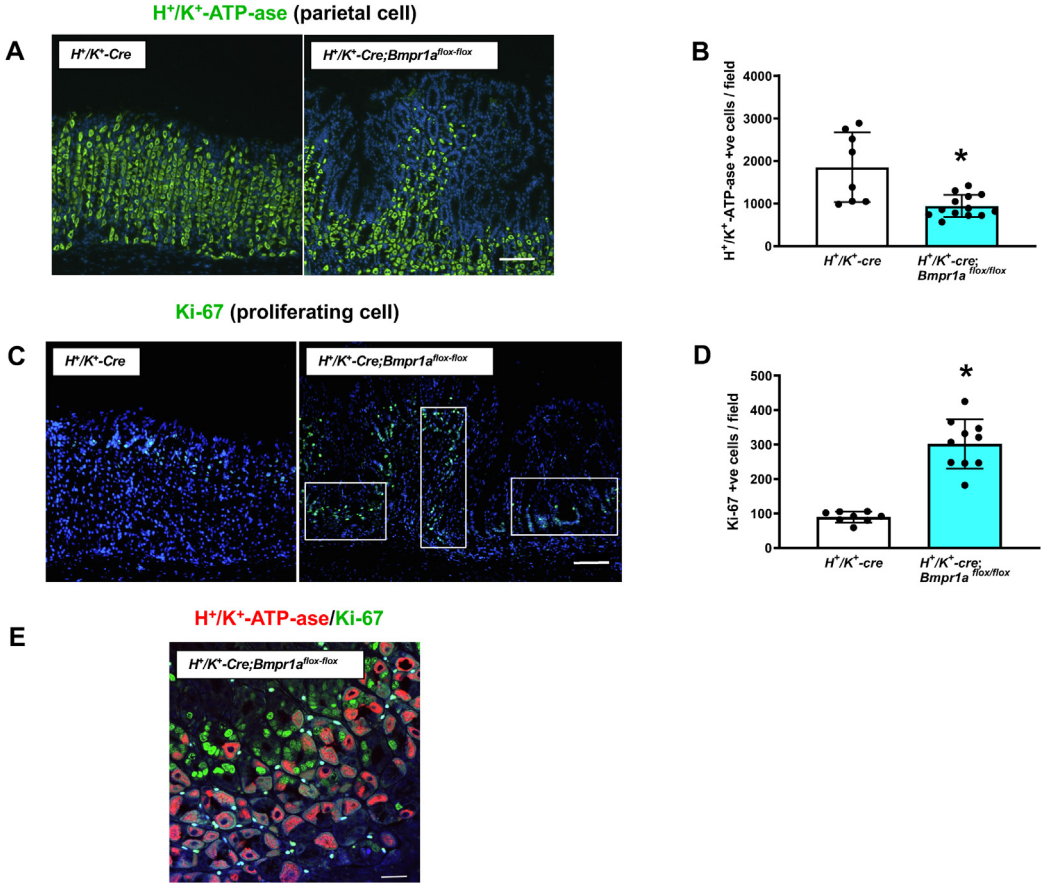

Figure 2. Decreased parietal cells and increased cell proliferation in six-month-old H^+/K^+-*Cre;Bmpr1a*$^{flox\text{-}flox}$ mice. Paraffin sections of the mucosa of the corpus of six-month-old H^+/K^+-*Cre* mice and of H^+/K^+-*Cre;Bmpr1a*$^{flox\text{-}flox}$ mice were stained with an anti-H^+,K^+-ATPase α-subunit primary antibody and an Alexa 488-conjugated secondary antibody (A) and with an anti-Ki-67 primary antibody and an Alexa 488-conjugated secondary antibody (C). Size bars 100 μm. Paraffin sections of the mucosa of the corpus of six-month-old H^+/K^+-*Cre;Bmpr1a*$^{flox\text{-}flox}$ mice were stained with an anti-H^+,K^+-ATPase α-subunit primary antibody and an Alexa 555-conjugated secondary antibody (red) together with an anti-Ki-67 primary antibody and an Alexa 488-conjugated secondary antibody (green) (E). Size bars 25 μm. Similar results were observed in at least 3 separate sections obtained from 4 separate mice. Windows frame glands exhibiting proliferating cells. Graph bars represent the number of H^+,K^+-ATPase α-subunit (B) and Ki-67 (D) positive cells detected in H^+/K^+-*Cre* mice and H^+/K^+-*Cre;Bmpr1a*$^{flox\text{-}flox}$ mice. Values are shown as means $\pm$ standard error. Numbers in parenthesis indicate the number of animals used in each group. *$P < .05$.

of parietal cells and chief cells were noted in sections obtained from three-month-old H^+K^+-*Cre;Bmpr1a*$^{flox\text{-}flox}$ mice which were stained with hematoxylin and eosin, anti-Ki-67, anti-H^+,K^+-ATPase α-subunit, and anti-IF antibodies (Figure A1).

To better define the cellular changes caused by the diminished expression of *Bmpr1a* in the parietal cells, we stained sections of the mucosa of both control and six-month-old H^+/K^+-*Cre;Bmpr1a*$^{flox\text{-}flox}$ mice with the lectins GSII and UEA1 which bind to neck and pit cell mucins, respectively. As shown in Figure 3A and B, H^+/K^+-*Cre;Bmpr1a*$^{flox\text{-}flox}$ mice demonstrated a marked downward expansion of the pit cell compartment with an increase in the number of UEA1-stained cells. In addition, we observed the presence of aberrant cells expressing GSII-positive mucins at the base of the glands of the corpus, indicating the development of SPEM in the gastric mucosa of H^+/K^+-*Cre;Bmpr1a*$^{flox\text{-}flox}$ mice.

In order to confirm the development of metaplasia, we stained sections of the gastric mucosa of six-month-old H^+/K^+-*Cre;Bmpr1a*$^{flox\text{-}flox}$ mice with antibodies directed against IF and with the lectin GSII. As shown in Figure 3C, H^+/K^+-*Cre;Bmpr1a*$^{flox\text{-}flox}$ mice displayed areas of the mucosa with cells that coexpressed markers of both mucus neck and zymogenic cell differentiation. In addition, staining of the sections with both anti-IF and anti-H^+,K^+-ATPase α-subunit antibodies revealed the presence of aberrant cells that exhibited markers of both parietal and zymogenic lineages (Figure 3D). Similar findings were also observed in the corpus of H^+/K^+-*Nog* mice (Figure 3E), which express the BMP inhibitor noggin in the oxyntic mucosa. Taken together, these observations suggest that diminished BMP signaling

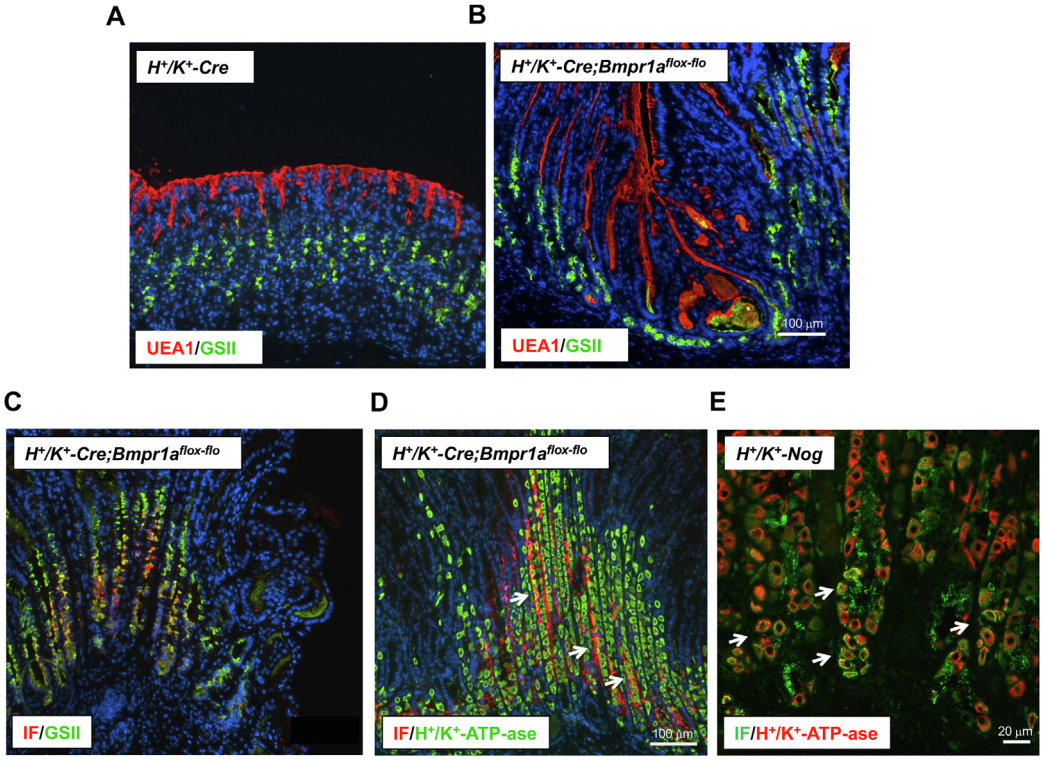

Figure 3. Cellular changes in the gastric mucosa of six-month-old H^+/K^+-*Cre;Bmpr1a*$^{flox\text{-}flox}$ mice. Paraffin sections of the gastric mucosa of the corpus of six-month-old H^+/K^+-*Cre* (A) and of H^+/K^+-*Cre;Bmpr1a*$^{flox\text{-}flox}$ mice (B) were stained with Alexa 555-conjugated UEA1 (red) and Alexa 488-conjugated GSII (green). Size bar 100 μm. Similar results were observed in at least 3 other mice from each group. (C) Paraffin sections of the gastric mucosa of the corpus of six-month-old H^+/K^+-*Cre;Bmpr1a*$^{flox\text{-}flox}$ mice were stained with anti-IF primary antibodies and Alexa 555-conjugated secondary antibodies (red) together with Alexa 488-conjugated GSII (green). (D) Paraffin sections of the gastric mucosa of the corpus of six-month-old H^+/K^+-*Cre;Bmpr1a*$^{flox\text{-}flox}$ mice were stained with anti-IF primary antibodies and Alexa 555-conjugated secondary antibodies (red) together with anti-H^+,K^+-ATPase α-subunit primary antibody and Alexa 488-conjugated secondary antibody (green). (E) Paraffin sections of the mucosa of the corpus of H^+/K^+-*Nog* mice were stained with anti-IF primary antibodies and Alexa 488-conjugated secondary antibodies (green) together with the anti-H^+,K^+-ATPase α-subunit primary antibody and Alexa 555-conjugated secondary antibody (red). Size bar 100 μm in (C) and (D) and 20 μm in (E). Similar results were observed in at least 3 other mice from each group. Arrows point to IF/H^+,K^+-ATPase α-subunit double-labeled cells.

leads to perturbations of the normal programs of parietal cell differentiation.

We sought to investigate BMP-regulated transcripts in the parietal cells in the presence and absence of BMP-generated signals. For these studies, we performed an RNA-Seq analysis using tomato-labeled parietal cells isolated, using flow-cytometry, from both noggin/tomato-expressing H^+/K^+-*Cre;*H^+/K^+-*Nog;Rosa26-Tom* (HKNT) mice and control HKT mice that express tomato but not noggin. In agreement with our previous observations,[13,15] noggin-expressing H^+/K^+-*Cre;*H^+/K^+-*Nog;Rosa26-Tom* mice exhibited a reduced number of parietal cells when compared to control H^+/K^+-*Cre;Rosa26-Tom* mice (Figure A2).

The RNA-seq analysis demonstrated 1249 upregulated genes and 897 downregulated genes in HKNT mice when compared to the control, HKT mice (Figure 4). The enrichment analysis of differentially expressed genes highlighted that the parietal cells of HKNT mice exhibit increased expression of molecules involved in the regulation of cellular apoptosis and in the response to inflammatory mediators, cellular stress, reactive oxygen species, Kirsten Rat Sarcoma viral oncogene homolog, and mammalian Target of Rapamycin Complex 1 signaling (Figure 5). In contrast, the parietal cells of HKNT mice showed down-regulation of genes involved in the response to hypoxia, protein secretion, and apical junction complex (Figure 6). To define more precisely the genetic landscape of the parietal cells in the presence of inhibition of BMP signaling, we performed a curated and more targeted analysis of parietal cell transcripts from HKNT mice. In these studies, we noted a significant increase in the expression of *Tff2*, *Muc6*, *Spdef*, and *Gif* genes that are normally expressed by mucus neck and zymogenic cells,[1,2,29] confirming the notion that diminished BMP signaling leads to the development of metaplastic gene signatures (Figure 7A). In support of this observation, we detected a significant induction of the SPEM markers, *GKN3*,[30,31] *Il1rn*, and *HE4/Wfdc2*,[32] and of the genes *Cd74*,[33] *Aqp5*,[34] *Il33*,[35] and *Pdgfa*,[36,37] which have been linked to gastric metaplasia and neoplasia

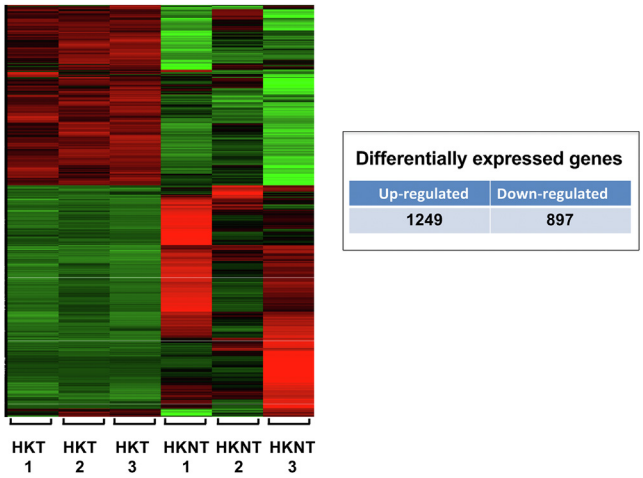

Figure 4. RNA-Seq analysis of transcripts of parietal cells isolated from *H*$^+$/*K*$^+$*-Cre;Rosa26-tdTom* (HKT) mice and *H*$^+$/*K*$^+$*-Nog;H*$^+$/*K*$^+$*-Cre;Rosa26-tdTom* (HKNT) mice. The heat map shows differentially regulated genes in *H*$^+$/*K*$^+$*-Cre;Rosa26-tdTom* (HKT) mice and *H*$^+$/*K*$^+$*-Nog;H*$^+$/*K*$^+$*-Cre;Rosa26-tdTom* (HKNT) mice. $P < .05$, $q < 0.05$.

(Figure 7A). Parietal cells of HKNT mice also exhibited decreased expression of AMPK (*Prkaa2*) (0.46-fold change, $P = .002$, $q = 0.02$) and PGC1α (*Ppargc1a*) (0.52-fold change, $P = .003$, $q = 0.02$), genes that belong to a recently described metabolic pathway that regulates parietal cell maturation and differentiation.[38]

To further confirm that parietal cells of HKNT mice express markers of metaplasia, we compared our RNA-seq data with previously identified gastric metaplasia (SPEM and intestinal Mmetaplasia) signature gene sets [27] and found, as shown in the Venn-diagram depicted in Figure 7B, that 9 out of the 36 genes reported in the published metaplasia gene set were significantly upregulated in the parietal cells of HKNT mice.

Discussion

In this manuscript, we report a series of novel observations that underscore the importance of BMP signaling in the regulation of parietal cell differentiation and gastric epithelial homeostasis. In particular, we demonstrate that

Description	Number of detected genes	Number of upregulated genes	P value
Genes up-regulated in response to interferon gamma	179	59	8.16E-23
Genes up-regulated in response to alpha interferon proteins	85	40	1.57E-22
Genes encoding proteins involved in oxidative phosphorylation	187	58	5.69E-21
A subgroup of genes regulated by MYC - version 1	186	45	2.97E-12
Genes involved in DNA repair	143	28	3.78E-06
Genes up-regulated by reactive oxigen species (ROS)	47	14	7.35E-06
Genes encoding components of the complement system, which is part of the innate immune system	178	30	3.78E-05
Genes encoding proteins involved in processing of drugs and other xenobiotics	195	31	8.86E-05
Genes involved in cholesterol homeostasis	71	15	2.76E-04
Genes defining late response to estrogen	193	29	3.93E-04
Genes up-regulated by KRAS activation	197	29	5.55E-04
Genes specifically up-regulated in pancreatic beta cells	39	10	5.72E-04
Genes regulated by NF-kB in response to TNF	192	28	7.96E-04
Genes up-regulated during adipocyte differentiation (adipogenesis).	194	28	9.38E-04
Genes involved in p53 pathways and networks.	194	28	9.38E-04
Genes mediating programmed cell death (apoptosis) by activation of caspases.	159	24	0.001126
Genes up-regulated through activation of mTORC1 complex.	197	28	0.001191
Genes encoding components of blood coagulation system; also up-regulated in platelets.	131	19	0.005492
Genes encoding proteins involved in glycolysis and gluconeogenesis.	197	25	0.009308
Genes up-regulated during unfolded protein response, a cellular stress response related to the endoplasmic reticulum	110	16	0.01002
Genes defining inflammatory response	190	23	0.02055
Genes involved in protein secretion pathway	91	13	0.02189

Figure 5. Gene Set Enrichment Analysis (GSEA) of parietal cell transcripts from *H*$^+$/*K*$^+$*-Cre;Rosa26-tdTom* (HKT) mice and *H*$^+$/*K*$^+$*-Nog;H*$^+$/*K*$^+$*-Cre;Rosa26-tdTom* (HKNT) mice. GSEA of upregulated transcripts in *H*$^+$/*K*$^+$*-Nog;H*$^+$/*K*$^+$*-Cre;Rosa26-tdTom* (HKNT) mice was performed using the Molecular Signatures Database v6 (MSigDB) Hallmark list. KRAS, Kirsten rat sarcoma viral oncogene homolog; TNF, Tumor necrosis factor; NF-κB, Nuclear factor-κB.

Description	Number of detected genes	Number of downregulated genes	P value
Genes down-regulated in response to ultraviolet (UV) radiation	143	23	3.64E-06
Genes involved in development of skeletal muscle (myogenesis)	194	24	0.000185
Genes defining response to androgens	96	15	0.000242
Genes encoding components of apical junction complex	192	23	0.0004
Genes involved in metabolism of heme (a cofactor consisting of iron and porphyrin) and erythroblast differentiation	185	22	0.000586
Genes defining early response to estrogen	193	22	0.001035
Genes up-regulated in response to TGFB1	52	9	0.002005
Genes important for mitotic spindle assembly	194	21	0.002525
Genes involved in protein secretion pathway	91	12	0.004286
Genes up-regulated in response to low oxygen levels (hypoxia)	191	19	0.009655

Figure 6. Gene Set Enrichment Analysis (GSEA) of parietal cell transcripts from *H^+/K^+-Cre;Rosa26-tdTom* (HKT) mice and *H^+/K^+-Nog;H^+/K^+-Cre;Rosa26-tdTom* (HKNT) mice. GSEA of downregulated transcripts in *H^+/K^+-Nog;H^+/K^+-Cre;Rosa26-tdTom* (HKNT) mice was performed using the Molecular Signatures Database v6 (MSigDB) Hallmark list. TGFB1, transforming growth factor beta.

specific inhibition of BMP signaling in the parietal cells causes profound morphological and functional changes of the fundic epithelium. Our studies indicate that the gastric mucosa of six-month-old *H^+/K^+-Cre;Bmpr1a$^{flox\text{-}flox}$* mice exhibits increased epithelial cell proliferation, paucity of parietal cells, and a marked expansion of the pit cell compartment which appears to extend downward toward the base of morphologically abnormal and compressed glands. The finding that these changes were detectable only in older mice is consistent with the previously described observation that the parietal cells exhibit a slow process of differentiation and maturation.[39]

One possible mechanism responsible for these changes could reflect the presence of increased expression of growth factors, such as epidermal growth factor receptor ligands, in the gastric mucosa of the transgenic mice. In support of this possibility, previously published reports from our laboratory have demonstrated that inhibition of BMP signaling by transgenic expression of noggin in the stomach leads to increased production of transformingrowth factor α and amphiregulin,[13] molecules known to stimulate cell proliferation and to promote pit cell differentiation.[40] Another plausible explanation could be related to the recently described ability of the parietal cells to contribute to the spatial organization of the glands of the fundus.[41] According to this theory, the parietal cells can direct the flow of cells that migrate from the stem cell zone of the isthmus to other sections of the glands while they complete their process of maturation and differentiation. It is conceivable that in our mice, the presence of scant and abnormal parietal cells that are unable to respond to BMP-generated signals might cause aberrancies in the normal mechanisms that regulate the process of cell migration and differentiation, leading to expansion of the pit cell compartment and to alterations in the normal spatial organization of the fundic mucosa.

In order to examine the consequences of inhibition of BMP signaling to the gene signature of the parietal cells, we performed an RNA-Seq analysis using pure populations of tomato-labeled parietal cells isolated from the gastric mucosa of noggin-expressing transgenic mice using flow cytometry. An enrichment analysis of parietal cell transcripts in the presence of noggin revealed a series of intriguing observations that demonstrate that inhibition of BMP signaling induces alterations in the normal genetic features of the parietal cells.

One interesting and novel finding of our study is that parietal cells exposed to noggin exhibit a significant increase in the expression of genes involved in inflammation, suggesting that BMP signaling plays an important role in the regulation of the response of the gastric mucosa to inflammatory stimuli. These observations support work from our laboratory that has shown that the noggin transgenic mice exhibit mucosal inflammation and an enhanced inflammatory response to *H. pylori*.[15] Another significant finding is that parietal cells of HKNT mice express gene signatures that can be detected in the context of both intestinal metaplasia and SPEM, supporting the notion that in the presence of inhibition of BMP-generated signals, the parietal cells exhibit decreased expression of markers of parietal cell differentiation and the acquisition of metaplastic gene signatures. In support of this hypothesis, we noted that parietal cells isolated from noggin-expressing mice demonstrate reduced expression of molecules such as AMPK and PGC1α which have been shown to direct progenitor cells to become differentiated parietal cells.[38] The concept that parietal cells can acquire metaplastic features was further substantiated by the observation that

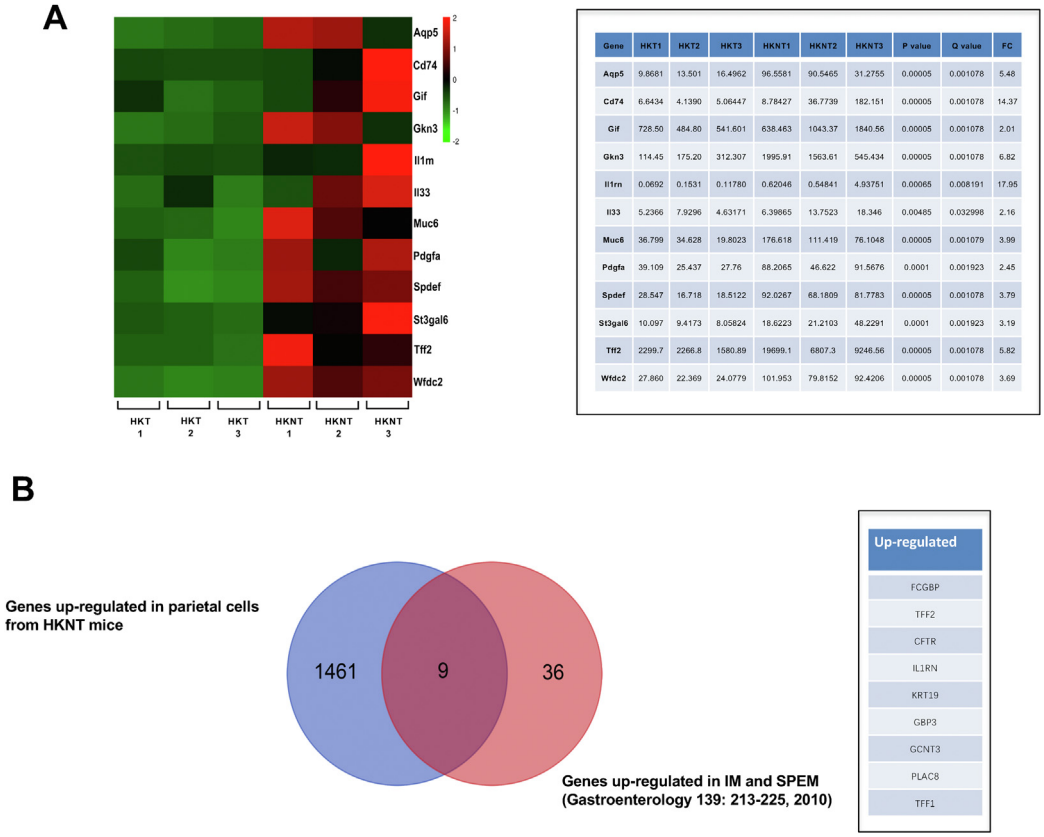

Gene	HKT1	HKT2	HKT3	HKNT1	HKNT2	HKNT3	P value	Q value	FC
Aqp5	9.8681	13.501	16.4962	96.5581	90.5465	31.2755	0.00005	0.001078	5.48
Cd74	6.6434	4.1390	5.06447	8.78427	36.7739	182.151	0.00005	0.001078	14.37
Gif	728.50	484.80	541.601	638.463	1043.37	1840.56	0.00005	0.001078	2.01
Gkn3	114.45	175.20	312.307	1995.91	1563.61	545.434	0.00005	0.001078	6.82
Il1rn	0.0692	0.1531	0.11780	0.62046	0.54841	4.93751	0.00065	0.008191	17.95
Il33	5.2366	7.9296	4.63171	6.39865	13.7523	18.346	0.00485	0.032998	2.16
Muc6	36.799	34.628	19.8023	176.618	111.419	76.1048	0.00005	0.001079	3.99
Pdgfa	39.109	25.437	27.76	88.2065	46.622	91.5676	0.0001	0.001923	2.45
Spdef	28.547	16.718	18.5122	92.0267	68.1809	81.7783	0.00005	0.001078	3.79
St3gal6	10.097	9.4173	8.05824	18.6223	21.2103	48.2291	0.0001	0.001923	3.19
Tff2	2299.7	2266.8	1580.89	19699.1	6807.3	9248.56	0.00005	0.001078	5.82
Wfdc2	27.860	22.369	24.0779	101.953	79.8152	92.4206	0.00005	0.001078	3.69

Figure 7. Metaplastic gene signatures in parietal cells of *H*$^+$/*K*$^+$-*Nog;H*$^+$/*K*$^+$-*Cre;Rosa26-tdTom* (HKNT) mice. (A) List of genes expressed in SPEM, involved in the regulation of cell proliferation and linked to the development of gastric neoplasia, which are upregulated in parietal cells of *H*$^+$/*K*$^+$-*Nog;H*$^+$/*K*$^+$-*Cre;Rosa26-tdTom* (HKNT) mice. (B) Venn diagram analysis depicting the overlap between transcripts expressed in our database and those listed in a published report of intestinal metaplasia- and SPEM-specific genes.[27] (C) List of shared genes.

inhibition of BMP signaling leads to the expression in the parietal cells of IF, a protein which, in mice, can be normally detected in chief cells.[1] Parietal cells of HKNT mice also displayed enhanced expression of genes associated with neoplastic transformation and cell proliferation, such as *Pdgfa*, a growth factor[36,37]; *Aqp5*, a molecule which labels antral stem cells and that appears to contribute to the development of gastric cancer[34]; and *Cd74*, a factor that is involved in the process of inflammation-linked gastric carcinogenesis.[33] Moreover, the data showed upregulation of genes induced by Ras signaling, a biochemical mechanism that has been shown to be responsible for the development of SPEM and the reprogramming of chief cells.[42,43] Taken together, these observations underscore the concept that inhibition of BMP signaling causes significant aberrations in parietal cell biology and mucosal homeostasis.

Another intriguing finding of the RNA-Seq analysis was that parietal cells isolated from HKNT mice exhibit increased expression of genes involved in mammalian Target Of Rapamycin Complex 1 signal transduction and in the folded protein response. Interestingly, these biochemical mechanisms have been linked to the endoplasmic reticulum stress response and to the induction of Paligenosis, a biological process in which cells challenged with stressful stimuli undergo reprogramming of their metabolic functions, regressing from a differentiated state to that of a dedifferentiated progenitor-like cell.[44,45] Thus, it is conceivable that in the presence of inhibition of BMP signaling, the tomato-labeled parietal cells could remain in a "transitional state" displaying features of immature, poorly differentiated cells.

One consideration that should be made in the interpretation of our data is that although the parietal cells of HKNT mice express metaplastic gene signatures, they do not appear to be proliferating. One possible explanation for this observation is that these parietal cells could give rise to nonproliferating metaplastic changes. Alternatively, it is conceivable that at least some of the proliferating cells might be the result of altered parietal cell differentiation, a process which could have led to the development of proliferating, immature epithelial cells that have failed to express detectable levels of markers of parietal cell differentiation. Future studies will be necessary to better define the mechanisms involved in these processes.

Conclusion

In conclusion, we demonstrated that inhibition of BMP signaling in the parietal cells leads to altered parietal

differentiation. These events appear to have broad repercussions on the homeostasis of the epithelium of the corpus which appears to undergo significant morphological and functional changes. Furthermore, we provide evidence that parietal cells devoid of BMP signals fail to differentiate normally, acquiring gene signatures that can be identified in the context of metaplasia. These findings underscore the importance of BMP signaling in the regulation of gastric homeostasis, and they provide new information regarding the pathophysiological mechanisms that lead to the development of metaplastic lesions of the stomach.

Supplementary Materials

Material associated with this article can be found in the online version at https://doi.org/10.1016/j.gastha.2022.10.002.

References

1. Willet SG, Mills JC. Stomach organ and cell lineage differentiation: from Embryogenesis to adult homeostasis. Cell Mol Gastroenterol Hepatol 2016;2:546–559.
2. Sáenz JB, Mills JC. Acid and the basis for cellular plasticity and reprogramming in gastric repair and cancer. Nat Rev Gastroenterol Hepatol 2018;15:257–273.
3. Del Valle J, Todisco A. Gastric secretion. In: Yamada T, ed. Textbook of gastroenterology. 3rd ed. Philadelphia: Lippincott, 1999:278–319.
4. Li Q, Karam SM, Gordon JI. Diphtheria toxin-mediated ablation of parietal cells in the stomach of transgenic mice. J Biol Chem 1996;271:3671–3676.
5. Canfield V, West AB, Goldenring JR, et al. Genetic ablation of parietal cells in transgenic mice: a new model for analyzing cell lineage relationships in the gastric mucosa. Proc Natl Acad Sci U S A 1996;93:2431–2435.
6. Goldenring JR, Ray GS, Coffey RJ, et al. Reversible drug-induced oxyntic atrophy in rats. Gastroenterology 2000;118:1080–1093.
7. Nomura S, Baxter T, Yamaguchi H, et al. Spasmolytic polypeptide expressing metaplasia to preneoplasia in H. felis-infected mice. Gastroenterology 2004;127:582–594.
8. Goldenring JR, Nomura S. Differentiation of the gastric mucosa III. Animal models of oxyntic atrophy and metaplasia. Am J Physiol Gastrointest Liver Physiol 2006;291:G999–G1004.
9. Petersen CP, Mills JC, Goldenring JR. Murine models of gastric corpus preneoplasia. Cell Mol Gastroenterol Hepatol 2017;3:11–26.
10. Nam KT, Lee HJ, Sousa JF, et al. Mature chief cells are cryptic progenitors for metaplasia in the stomach. Gastroenterology 2010;139:2028–2037.
11. Radyk MD, Burclaff J, Willet SG, et al. Metaplastic cells in the stomach Arise, independently of stem cells, via dedifferentiation or transdifferentiation of chief cells. Gastroenterology 2018;154:839–843.
12. Todisco A. Regulation of gastric metaplasia, dysplasia, and neoplasia by bone morphogenetic protein signaling. Cell Mol Gastroenterol Hepatol 2017;3:339–347.
13. Shinohara M, Mao M, Keeley TM, et al. Bone morphogenetic protein signaling regulates gastric epithelial cell development and proliferation in mice. Gastroenterology 2010;139:2050–2060.e2.
14. Nitsche H, Ramamoorthy S, Sareban M, et al. Functional role of bone morphogenetic protein-4 in isolated canine parietal cells. Am J Physiol Gastrointest Liver Physiol 2007;293:G607–G614.
15. Takabayashi H, Shinohara M, Mao M, et al. Anti-inflammatory activity of bone morphogenetic protein signaling pathways in stomachs of mice. Gastroenterology 2014;147:396–406.
16. Barker N, Huch M, Kujala P, et al. Lgr5+ve stem cells drive Self-Renewal in the stomach and Build Long-Lived gastric Units in Vitro. Cell Stem Cell 2010;6:25–36.
17. Mishina Y, Hanks MC, Miura S, et al. Generation of Bmpr/Alk3 conditional knockout mice. Genesis 2002;32:69–72.
18. Syder AJ, Karam SM, Mills JC, et al. A transgenic mouse model of metastatic carcinoma involving transdifferentiation of a gastric epithelial lineage progenitor to a neuroendocrine phenotype. Proc Natl Acad Sci 2004;101:4471–4476.
19. Todisco A, Mao M, Keeley TM, et al. Regulation of gastric epithelial cell homeostasis by gastrin and bone morphogenetic protein signaling. Physiol Rep 2015;3:e12501.
20. Demitrack ES, Gifford GB, Keeley TM, et al. Notch signaling regulates gastric antral LGR5 stem cell function. EMBO J 2015;34:2522–2536.
21. Eaton KA, Danon SJ, Krakowka S, et al. A reproducible scoring system for quantification of histologic lesions of inflammatory disease in mouse gastric epithelium. Comp Med 2007;57:57–65.
22. Schindelin J, Arganda-Carreras I, Frise E, et al. An open-source platform for biological-image analysis. Nat Methods 2012;28:676–682.
23. Langmead B, Trapnell C, Pop M, et al. Ultrafast and memory efficient alignment of short DNA sequences to the human genome. Genome Biol 2009;10:R25.
24. Trapnell C, Pachter L, Salzberg SL. (2009). TopHat: discovering splice junctions with RNA-Seq. Bioinformatics 2009;25:1105–1111.
25. Trapnell C, Hendrickson D, Sauvageau S, et al. Differential analysis of gene regulation at transcript resolution with RNA-seq. Nat Biotechnol 2013;31:46–53.
26. Liberzon A, Birger C, Thorvaldsdottir H, et al. The molecular signatures database Hallmark gene set collection. Cell Syst 2015;1:417–425.
27. Lee HJ, Nam KT, Park HS, et al. Gene expression profiling of metaplastic lineages identifies CDH17 as a prognostic marker in early stage gastric cancer. Gastroenterology 2010;139:213–225.e3.
28. Miyazono K, Maeda S, Imamura T. BMP receptor signaling: transcriptional targets, regulation of signals, and signaling cross-talk. Cytokine Growth Factor Rev 2005;16:251–263.
29. Horst D, Gu X, Bhasin M, et al. Requirement of the epithelium-specific Ets transcription factor Spdef for mucous gland cell function in the gastric antrum. J Biol Chem 2010;285:35047–35055.
30. Menheniott TR, Peterson AJ, O'Connor L, et al. A novel gastrokine, Gkn3, marks gastric atrophy and shows evidence of adaptive gene loss in humans. Gastroenterology 2010;138:1823–1835.

31. Bockerstett KA, Lewis SA, Noto CN, et al. Single-cell transcriptional analyses identify lineage-specific epithelial responses to inflammation and metaplastic development in the gastric corpus. Gastroenterology 2020; 159:2116–2129.
32. Koji Nozaki K, Masako Ogawa M, Janice A, et al. A molecular signature of gastric metaplasia arising in response to acute parietal cell loss. Gastroenterology 2008;134:511–522.
33. Beswick EJ, Reyes VE. CD74 in antigen presentation, inflammation, and cancers of the gastrointestinal tract. World J Gastroenterol 2009;15:2855–2861.
34. Tan SH, Swathi Y, Tan S, et al. AQP5 enriches for stem cells and cancer origins in the distal stomach. Nature 2020;578:437–443.
35. Petersen CP, Meyer AR, De Salvo C, et al. A signalling cascade of IL-33 to IL-13 regulates metaplasia in the mouse stomach. Gut 2018;67:805–817.
36. Chan F, Liu Y, Sun H, et al. Distribution and possible role of PDGF-AA and PDGFR-alpha in the gastrointestinal tract of adult Guinea pigs. Virchows Arch 2010;457:381–388.
37. Huang F, Wang D, Yao Y, et al. PDGF signaling in cancer progression. Int J Clin Exp Med 2017;10:9918–9929.
38. Miao ZF, Adkins-Threats M, Burclaff JR, et al. A Metformin-responsive metabolic pathway controls distinct Steps in gastric progenitor fate decisions and maturation. Cell Stem Cell 2020;26:910–925.
39. Keeley TK, Samuelson LC. Cytodifferentiation of the postnatal mouse stomach in normal and Huntingtin-interacting protein 1-related-deficient mice. Am J Physiol Gastrointest Liver Physiol 2010;299:G1241–G1251.
40. WÖlffling S, Daddi AA, Imai-Matsushima A, et al. EGF and BMPs govern differentiation and patterning in human gastric. Gastroenterology 2021;161:623–636.
41. Han S, Fink J, Jörg DJ, et al. Defining the identity and dynamics of adult gastric isthmus stem cells. Cell Stem Cell 2019;25:342–356.
42. Choi E, Hendley AM, Bailey JM, et al. Expression of activated Ras in gastric chief cells of mice leads to the full spectrum of metaplastic lineage transitions. Gastroenterology 2016;150:918–930.
43. Min J, Vega PN, Engevik AC, et al. Heterogeneity and dynamics of active Kras-induced dysplastic lineages from mouse corpus stomach. Nat Commun 2019;10:5549.
44. Miao ZF, Lewis MA, Cho CJ, et al. A dedicated evolutionarily conserved molecular network licenses differentiated cells to return to the cell cycle. Dev Cell 2020;55:178–194.
45. Willet SG, Lewis MA, Miao ZF, et al. Regenerative proliferation of differentiated cells by mTORC1-dependent paligenosis. EMBO J 2018;37:e98311.

Received January 23, 2022. Accepted October 4, 2022.

Correspondence:
Address correspondence to: Andrea Todisco, MD, 6520 MSRB I, Ann Arbor, Michigan 48109-0682. e-mail: atodisco@umich.edu.

Acknowledgments:
The authors thank Kathy McClinchey for assistance with tissue processing, the University of Michigan Flow Cytometry Core for assistance with cell sorting, and Rork Kuick and the University of Michigan Advanced Genomics and Bioinformatics Cores for assistance with the RNA-Seq studies.

Authors' Contributions:
Hidehiko Takabayashi: Study concept and design, acquisition of data, analysis and interpretation of data, critical revision of the manuscript, statistical analysis. Tuo Ji: Study concept and design, acquisition of data, analysis and interpretation of data, critical revision of the manuscript, statistical analysis. Maria Mao: Acquisition of data, analysis and interpretation of data, technical support, statistical analysis. Masahiko Shinohara: Acquisition of data, analysis and interpretation of data, technical support, statistical analysis. Kathryn A. Eaton: Acquisition, analysis and interpretation of data, critical revision of the manuscript for important intellectual content. Yatrik M. Shah: Analysis and interpretation of data, critical revision of the manuscript for important intellectual content, obtained funding. Andrea Todisco: Study concept and design, acquisition of data, analysis and interpretation of data, critical revision of the manuscript for important intellectual content; statistical analysis, obtained funding, study supervision, writing of the manuscript.

Conflicts of Interest:
The authors disclose no conflicts.

Funding:
This work was supported by RO1DK121785 (to A. Todisco), the University of Michigan Center for Gastrointestinal Research (grant P30-DK-34933), RO1CA148828 (Y. M. Shah), RO1CA245546 (Y. M. Shah), RO1DK095201 (Y. M. Shah), and the Department of Defense (CA171086) (Y. M. Shah).

Ethical Statement:
The corresponding author, on behalf of all authors, jointly and severally, certifies that their institution has approved the protocol for any investigation involving humans or animals and that all experimentation was conducted in conformity with ethical and humane principles of research.

Data Transparency Statement:
The data, analytic methods, and materials used in this study will be freely available to other researchers according to NIH Policy on Sharing of Model Organisms for Biomedical Research, Contracts on Obtaining and Disseminating Biomedical Research Resources and the NIH Grants Policy Statement.

Reporting Guidelines:
Care and Use of Laboratory Animals, SAGER.